JOURNAL OF MATERIALS SCIENCE **35** (2000) 3727–3732

Predicted calcium titanate solution mechanisms in calcium aluminoferrite and related phases

M. O. ZACATE, R. W. GRIMES
Department of Materials, Imperial College of Science, Technology, and Medicine, Prince Consort Road, London SW7 2BP, UK
E-mail: r.w.grimes@ic.ac.uk

K. SCRIVENER
Laboratoire Central de Recherche, Lafarge, 38291 St. Quentin Fallavier, France

Computer simulation, using an ionic, Born-like model, is used to investigate the accommodation of titanium impurities in Ca-Al-Fe-O phases. Specifically, calcium titanate solution in Al_2O_3, Fe_2O_3, CF, C_2F, CA, C_2A, C_3A, and C_4AF (where C denotes CaO) is considered. The simulations predict that titanium impurities are found preferentially in the ferrite phases. At sufficiently high concentrations, the solution involves the formation of clusters containing 3 to 6 ions that strongly resemble the structure of the calcium titanate phase. The calculations reveal that the compensation mechanism varies appreciably over the range of compounds considered.

1. Introduction

Ferrite phases constitute a substantial proportion of both calcium aluminate and Portland cements. In both cases there is substantial solid solution of other elements, present as impurities in the raw materials. It is highly likely that such impurities may affect the reactivity of these phases. Additionally, it has been shown in calcium aluminate cements [1, 2] that titanium plays a major role in the exsolution of the ferrite into two crystalline forms, one based on brownmillerite and the other based on perovskite. Determination of the complex mineralogy of these cements is an important element in the determination of the phase proportions by X-Ray diffraction [3]. However, in the aluminate and ferrite phases, titanium impurities are accompanied by silicon and magnesium impurities [4]. The presence of magnesium and silicon makes it difficult to evaluate the effect that titanium alone has on the defect chemistry of these compounds. To better understand the role of titanium, the lowest energy mechanisms for the accommodation of titanium in Al_2O_3, Fe_2O_3, CF, C_2F, CA, C_2A, C_3A, and C_4AF (where C, A and F denotes CaO, Al_2O_3 and Fe_2O_3 respectively) are determined by computer simulation with special attention given to the ferrite phases, $Ca_2Al_2O_5$ (C_2A), $Ca_2Fe_2O_5$ (C_2F) and Ca_2FeAlO_5 (C_4AF). Based on observations of cement chemistry, titanium solution was calculated exclusively with respect to $CaTiO_3$ (CT) since free TiO_2 is not observed and an excess of free lime is generally available for the formation of CT.

2. Methodology

2.1. Solution reactions

The energies of CT solution in the selected phases are determined in the usual way: for a given solution reaction, energies of the reactants are subtracted from the energies of the products. For example, a possible reaction for CT solution in α-Al_2O_3 is

$$CT \rightarrow Ca'_{Al} + Ti^{\bullet}_{Al} + 3O^{\times}_{O}.$$

Whole formula units such as CT in the above reaction have energies that are determined according to the perfect lattice energy calculations described below. Defects, represented by Kröger-Vink notation (for example, Ca'_{Al} and $Ti^{\bullet}_{Al}$ above), have energies determined by the defect calculations also described below. The energy of such a defect is the difference between the energy of the lattice with and without the defect. Therefore, a host ion sitting in the correct lattice position (for example, $O^{\times}_{O}$ above) corresponds to zero defect energy.

As a result of CT solution, one or more formula units of host lattice ions are displaced, i.e. the solute ions replace the host lattice ions. The displaced ions form new lattice on the surface and increase the overall volume of host lattice. Thus new units of host lattice form which also have to be accounted for energetically. The number of units formed can be determined by considering the subscripts of the defects in the solution reaction. In the example above, there are two aluminum lattice sites created (Ca'_{Al} and $Ti^{\bullet}_{Al}$) and three oxygen sites formed ($3O^{\times}_{O}$), thus the lattice energy of one Al_2O_3 unit must be included in the determination of the solution energy.

In some reactions, Fe^{3+} ions undergo reduction to Fe^{2+}. When this occurs, there is a purely electronic contribution to the reaction, and the third ionization energy of iron must be subtracted. This value is site dependent because the Fe 3d orbitals are split differently in an octahedral site compared to a tetrahedral site [5]. Often associated with the reduction of Fe^{3+} is

TABLE I Physical constants

quantity	value
$Fe^{2+} \rightarrow e^- + Fe^{3+}$ (III ionization energy)	
In an octahedral site	31.168 eV*
In a tetrahedral site	30.995 eV*
$\frac{1}{2}O_2 \rightarrow O$ (dissociation)	2.563 eV†
$O + e^- \rightarrow O^-$ (first e^- affinity)	−1.461 eV‡
$O^- + e^- \rightarrow O^{2-}$ (second e^- affinity)	8.8 eV§

* the in-crystal electronic contribution, references [13] and [5].
† reference [14]
‡ reference [13]
§This value is based on the value needed on average to complete the Born-Haber cycle using the calculated lattice energy and experimental values for the other quantities of the compounds in this study. For a discussion of the meaning of the second electron affinity of oxygen, see Harding and Pyper [15] and Grimes, Binks and Lidiard [16].

the evolution of oxygen. When this happens, there are three energy terms that must be included: the dissociation of O_2, and the first and second electron affinities of oxygen (i.e. $\frac{1}{2}O_2 + 2e^- \rightarrow O^{2-}$). The values used for these additional quantities are summarized in Table I.

2.2. Calculation of interatomic energies

To calculate the perfect lattice and defect energies, a Born-like model is used in which the ions assume their formal charges. In this approximation, the lattice energy arises from three sources: Coulombic interactions between ions, a shell model description of atomic polarization, and an additional interaction between ion pairs described by parameterised short-range forces that account for electron cloud overlap and dispersion forces. In these calculations, the Coulombic forces are summed using Ewald's method to provide convergence. The shell model approximates atomic polarization by modelling each polarizable ion as a massless shell of charge Y that is able to move with respect to a massive core with charge X, subject to a restraining harmonic force constant k [6]. To represent the short-range interactions, ion pairs interact through Buckingham potentials

$$E_{ij}(r) = A_{ij}e^{-r/\rho_{ij}} - C_{ij}/r^6$$

where r is the distance between the two atomic species (each cation–anion pair and the anion–anion pair) and A_{ij}, ρ_{ij}, and C_{ij} are adjustable parameters specific to each pair of ions i and j. The magnitude of this interaction falls off quickly with increasing r, and only ions separated within a certain cut-off distance (17.52 Å in this study) are considered.

2.3. Perfect lattice calculations

The perfect lattice energy is determined by starting with the experimentally determined structure and then adjusting both ion positions and lattice vectors, using the Newton-Raphson minimization procedure, until each ion experiences zero force. The short-range potential parameters are chosen so that the structure resulting from energy minimization reproduces the experimentally determined structure as closely as possible. The

TABLE II Potential parameters

short-range potentials	reference		
O^{2-}–O^{2-}	A	9547.96 eV	[7–9]
	ρ	0.21916 Å^{-1}	
	C	32.0 eVÅ^6	
Al^{3+}–O^{2-}	A	1725.2 eV	[7]
	ρ	0.28971 Å^{-1}	
	C	0.0 eVÅ^6	
Fe^{3+}–O^{2-}	A	1414.6 eV	[8]
	ρ	0.3128 Å^{-1}	
	C	0.0 eVÅ^6	
Fe^{2+}–O^{2-}	A	835.5 eV	[8]
	ρ	0.3288 Å^{-1}	
	C	0.0 eVÅ^6	
Ca^{2+}–O^{2-}	A	1186.48 eV	[7]
	ρ	0.339 Å^{-1}	
	C	0.0 eVÅ^6	
Sr^{2+}–O^{2-}	A	682.7 eV	[9]
	ρ	0.3945 Å^{-1}	
	C	0.0 eVÅ^6	
Ti^{4+}–O^{2-}	A	2131.04 eV	this work
	ρ	0.3038 Å^{-1}	
	C	0.0 eVÅ^6	
shell model parameters			
O^{2-}	Y	−2.80 $\|e\|$	[7–9, 17]
	X	0.80 $\|e\|$	
	k	54.8 eVÅ^{-2}	

set of short-range potential parameters are constrained to be the same for every structure in the study. This results in a parameter set that is capable of describing the potential energy between two ions not only at equilibrium but over a range of separations and a variety of coordinations. This is essential for modelling the structural relaxation around point defects. Nevertheless, the methodology is approximate, and one should compare relative disorder and solution energies in the various materials rather than base an analysis on absolute energies.

The short-range potential parameters (Table II) for the host materials of this study have been shown to successfully reproduce the lattice parameters of Al_2O_3, Fe_2O_3, CaO, CA, C_2A, C_3A, CA_2, CA_6, CF, C_2F, and C_4AF [7]. The Ca^{2+}–O^{2-} parameters were chosen specifically for that study. The Fe^{3+}–O^{2-}, Al^{3+}–O^{2-}, and O^{2-}–O^{2-} parameters were also developed to reproduce a large variety of structures, this data being summarised in Zacate and Grimes [7]. Two of those studies [8, 9] are the sources of the Fe^{2+}–O^{2-} and Sr^{2+}–O^{2-} potential parameters.

The Ti^{4+}–O^{2-} parameters have been modified slightly from a study of $SrTiO_3$ interfaces [9]. They have been chosen to reproduce the mixed oxide structural parameters of Table III as closely as possible, and are therefore unsuitable for modelling TiO_2 polymorphs. However, the potential set reproduces the structures of $SrTiO_3$, ilmenite ($FeTiO_3$), and CT very well. The agreement with the experimental structures of Al_2TiO_5 and pseudobrookite (Fe_2TiO_5) is also acceptable. Thus, the Ti^{4+}–O^{2-} parameters describe Ti^{4+} in a variety of crystallographic environments—necessary for modelling the relaxation around Ti^{4+} impurities in cement phases.

TABLE III Summary of structural parameters of mixed oxides containing titanium*

compound	property	calculated	observed	percent agreement	reference
$SrTiO_3$	*a* (Å)	3.917	3.905	100.30	[18]
$FeTiO_3$	*a* (Å)	5.121	5.088	100.65	[19]
	c (Å)	14.07	14.09	99.87	
$CaTiO_3$	*a* (Å)	5.4113	5.4458	99.37	[20]
	b (Å)	7.6458	7.6453	100.01	
	c (Å)	5.4068	5.3829	100.44	
Fe_2TiO_5	*a* (Å)	3.61	3.72	97.04	[21]
	b (Å)	9.94	9.79	101.58	
	c (Å)	9.96	9.93	100.26	
Al_2TiO_5	*a* (Å)	3.502	3.591	97.51	[22]
	b (Å)	9.556	9.429	101.34	
	c (Å)	9.768	9.636	101.37	

*significant figures from references

2.4. Defect calculations

To calculate the enthalpy of a defect, such as a vacancy, an interstitial ion, or a substitutional ion, the Mott-Littleton approach is used [10]. This method begins with the relaxed perfect lattice and then places a defect in the centre of a spherical region I. All ion positions in region I are allowed to relax in response to the defect, and interactions are summed over all pairs of ions within the region. The radius of region I in these calculations is 11.68 Å. Larger radius values than this make negligible difference to predicted defect energies. The outer region, region IIb, extends to infinity and the interaction of the region IIb ions with the lattice defect is treated as a dielectric response in accord with the Mott-Littleton approximation. To ensure a smooth transition between regions I and IIb, an interfacial region, region IIa, is introduced. The relaxation of ion positions within region IIa is determined within the Mott-Littleton approximation (i.e. ions are subject to forces approximated assuming a dielectric response); however, interaction energies between ions in region IIa and region I are calculated explicitly. Consequently the radius of region IIa must be greater than that of region I by more than the short-range interaction cut-off distance defined earlier (see Section 2.2). The region IIa radius in these calculations is 29.6 Å, and the whole procedure is executed with the CASCADE code [11].

3. Results

The results are presented in three sections. First, the lowest energy solution reactions for the non-ferrite phases (Al_2O_3, Fe_2O_3, CF, CA, and C_3A) are considered. Then, the solution mechanisms for three stoichiometries of the ferrite phase (C_2A, C_4AF, and C_2F) are considered in greater detail. Finally, defect clustering in C_4AF and C_2F is examined.

In each of the host materials considered below, one can envisage many possible solution mechanisms associated with different charge compensating defects. The majority of these have highly unfavourable energies. For example, except for those reported, other reaction mechanisms involving vacancies or cation interstitials have solution energies anywhere from 6 eV to 24 eV per titanium ion incorporated. For conciseness, only the lowest energy solution reactions are reported. Furthermore solution mechanisms in which titanium substitutes for calcium will not be included because it is clear that a small highly charged ion such as titanium would be unlikely to substitute for a large substantially lower charged ion such as calcium.

3.1. Non-ferrite phases

In each case below, the total solution energy is given. To compare different mechanisms, it is necessary to normalize the energies (solution energy per CT formula unit, for example).

- α-Al_2O_3

$$2\mathrm{CT} \xrightarrow{\Delta H = 9.48\,\mathrm{eV}} 2\mathrm{Ti}_{\mathrm{Al}}^{\bullet} + \mathrm{O}_{\mathrm{i}}'' + 3\mathrm{O}_{\mathrm{O}}^{\times} + 2\mathrm{CaO}$$

$$\mathrm{CT} \xrightarrow{\Delta H = 4.69\,\mathrm{eV}} \mathrm{Ca}_{\mathrm{Al}}' + \mathrm{Ti}_{\mathrm{Al}}^{\bullet} + 3\mathrm{O}_{\mathrm{O}}^{\times}$$

- α-Fe_2O_3

$$2\mathrm{CT} \xrightarrow{\Delta H = 8.00\,\mathrm{eV}} 2\mathrm{Ti}_{\mathrm{Fe}}^{\bullet} + \mathrm{O}_{\mathrm{i}}'' + 3\mathrm{O}_{\mathrm{O}}^{\times} + 2\mathrm{CaO}$$

$$\mathrm{CT} \xrightarrow{\Delta H = 2.93\,\mathrm{eV}} \mathrm{Ca}_{\mathrm{Fe}}' + \mathrm{Ti}_{\mathrm{Fe}}^{\bullet} + 3\mathrm{O}_{\mathrm{O}}^{\times}$$

$$2\mathrm{CT} + 2\mathrm{Fe}_{\mathrm{Fe}}^{\times} \xrightarrow{\Delta H = 4.65\,\mathrm{eV}} 2\mathrm{Ti}_{\mathrm{Fe}}^{\bullet} + 2\mathrm{Fe}_{\mathrm{Fe}}' + 3\mathrm{O}_{\mathrm{O}}^{\times} + 2\mathrm{CaO} + \tfrac{1}{2}\mathrm{O}_2$$

- CA

$$2\mathrm{CT} \xrightarrow{\Delta H = 7.58\,\mathrm{eV}} \mathrm{Ca}_{\mathrm{Ca}}^{\times} + 2\mathrm{Ti}_{\mathrm{Al}}^{\bullet} + 4\mathrm{O}_{\mathrm{O}}^{\times} + \mathrm{O}_{\mathrm{i}}'' + \mathrm{CaO}$$

- CF

$$2\mathrm{CT} \xrightarrow{\Delta H = 7.78\,\mathrm{eV}} \mathrm{Ca}_{\mathrm{Ca}}^{\times} + 2\mathrm{Ti}_{\mathrm{Fe}}^{\bullet} + 4\mathrm{O}_{\mathrm{O}}^{\times} + \mathrm{O}_{\mathrm{i}}'' + \mathrm{CaO}$$

$$2\mathrm{CT} + 2\mathrm{Fe}_{\mathrm{Fe}}^{\times} \xrightarrow{\Delta H = 3.55\,\mathrm{eV}} \mathrm{Ca}_{\mathrm{Ca}}^{\times} + 2\mathrm{Ti}_{\mathrm{Fe}}^{\bullet} + 2\mathrm{Fe}_{\mathrm{Fe}}' + 4\mathrm{O}_{\mathrm{O}}^{\times} + \mathrm{CaO} + \tfrac{1}{2}\mathrm{O}_2$$

- C_3A

$$2\mathrm{CT} \xrightarrow{\Delta H = 5.52\,\mathrm{eV}} 2\mathrm{Ca}_{\mathrm{Ca}}^{\times} + \mathrm{V}_{\mathrm{Ca}}'' + 2\mathrm{Ti}_{\mathrm{Al}}^{\bullet} + 6\mathrm{O}_{\mathrm{O}}^{\times}$$

In all the above phases, titanium substitutes for the trivalent host cation. In the phases which contain iron, reduction of Fe^{3+} to Fe^{2+} is favoured so that Fe_{Fe}' is the compensating defect. In alumina, the compensating defect is Ca_{Al}'. In CA, oxygen interstitials compensate titanium substitution. Finally, in C_3A, calcium vacancies provide the lowest energy compensation.

3.2. The ferrite phase

In this section, the solution of calcium titanate in the ferrite phase is considered in detail. In particular, the

solution reactions are written to distinguish the crystallographic sites occupied by the titanium so that "(o)" denotes the octahedral site and "(t)" represents the tetrahedral site. The effect of reducing environments on solution in C_2F and C_4AF is also considered.

The basic solution reactions are as follows:

- C_2A

$$2CT \xrightarrow{\Delta H = 5.54\,eV} 2Ca_{Ca}^{\times} + Ti_{Al(o)}^{\bullet} + Ti_{Al(t)}^{\bullet} + 5O_O^{\times} + O_i''$$

- C_2F

$$2CT + 2Fe_{Fe(t)}^{\times} \xrightarrow{\Delta H = 5.35\,eV} 2Ca_{Ca}^{\times} + 2Fe_{Fe(t)}' + Ti_{Fe(o)}^{\bullet} + Ti_{Fe(t)}^{\bullet} + 5O_O^{\times} + \tfrac{1}{2}O_2$$

$$2CT \xrightarrow{\Delta H = 4.90\,eV} 2Ca_{Ca}^{\times} + Ti_{Fe(o)}^{\bullet} + Ti_{Fe(t)}^{\bullet} + 5O_O^{\times} + O_i''$$

- C_4AF

$$2CT + 2Fe_{Fe(o)}^{\times} \xrightarrow{\Delta H = 6.41\,eV} 2Ca_{Ca}^{\times} + 2Fe_{Fe(o)}' + Ti_{Fe(o)}^{\bullet} + Ti_{Al(t)}^{\bullet} + 5O_O^{\times} + \tfrac{1}{2}O_2$$

$$2CT \xrightarrow{\Delta H = 6.92\,eV} Ca_{Ca}^{\times} + Ti_{Fe(o)}^{\bullet} + Ti_{Al(t)}^{\bullet} + 5O_O^{\times} + V_{Ca}'' + CaO$$

$$2CT \xrightarrow{\Delta H = 5.40\,eV} 2Ca_{Ca}^{\times} + Ti_{Fe(o)}^{\bullet} + Ti_{Al(t)}^{\bullet} + 5O_O^{\times} + O_i''$$

The distinction between octahedral and tetrahedral sites is important because there is an appreciable difference in defect energy for titanium at an octahedral versus a tetrahedral site. Consistently, lower energy solution mechanisms are obtained when the titanium is located only at octahedral sites. The following reactions exploit this by requiring that titanium occupies only octahedral sites.

- C_2A

$$2CT + Al_{Al(o)}^{\times} \xrightarrow{\Delta H = 3.30\,eV} 2Ca_{Ca}^{\times} + 2Ti_{Al(o)}^{\bullet} + Al_{Al(t)}^{\times} + 5O_O^{\times} + O_i''$$

- C_2F

$$2CT + 2Fe_{Fe(t)}^{\times} + Fe_{Fe(o)}^{\times} \xrightarrow{\Delta H = 3.48\,eV} 2Ca_{Ca}^{\times} + 2Fe_{Fe(t)}' + 2Ti_{Fe(o)}^{\bullet} + Fe_{Fe(t)}^{\times} + 5O_O^{\times} + \tfrac{1}{2}O_2$$

$$2CT + Fe_{Fe(o)}^{\times} \xrightarrow{\Delta H = 3.02\,eV} 2Ca_{Ca}^{\times} + 2Ti_{Fe(o)}^{\bullet} + Fe_{Fe(t)}^{\times} + 5O_O^{\times} + O_i''$$

- C_4AF

$$2CT + 3Fe_{Fe(o)}^{\times} \xrightarrow{\Delta H = 4.46\,eV} 2Ca_{Ca}^{\times} + 2Fe_{Fe(o)}' + 2Ti_{Fe(o)}^{\bullet} + Fe_{Al(t)}^{\times} + 5O_O^{\times} + \tfrac{1}{2}O_2$$

$$2CT + Fe_{Fe(o)}^{\times} \xrightarrow{\Delta H = 4.96\,eV} Ca_{Ca}^{\times} + 2Ti_{Fe(o)}^{\bullet} + Fe_{Al(t)}^{\times} + 5O_O^{\times} + V_{Ca}'' + CaO$$

$$2CT + 2Fe_{Fe(o)}^{\times} + Al_{Al(t)}^{\times} \xrightarrow{\Delta H = 4.04\,eV} 2Ca_{Ca}^{\times} + 2Fe_{Al(t)}' + 2Ti_{Fe(o)}^{\bullet} + Al_{Fe(o)}^{\times} + 5O_O^{\times} + \tfrac{1}{2}O_2$$

$$2CT + Fe_{Fe(o)}^{\times} \xrightarrow{\Delta H = 3.44\,eV} 2Ca_{Ca}^{\times} + 2Ti_{Fe(o)}^{\bullet} + Fe_{Al(t)}^{\times} + 5O_O^{\times} + O_i''$$

At all three stoichiometries of the ferrite phase, the lowest energy solution reaction occurs when oxygen interstitials are the compensating defects.

To understand solution under reducing conditions, it is necessary to assume that the defects formed due to the reduction process are already present. When C_2F is reduced

$$2Fe_{Fe(t)}^{\times} \longrightarrow V_O^{\bullet\bullet} + 2Fe_{Fe(t)}' + \tfrac{1}{2}O_2$$

and when C_4AF is reduced

$$2Fe_{Fe(o)}^{\times} + 2Al_{Al(t)}^{\times} \longrightarrow V_O^{\bullet\bullet} + 2Al_{Fe(o)}^{\times} + 2Fe_{Al(t)}' + \tfrac{1}{2}O_2.$$

Thus, oxygen vacancies are present in the reduced materials. Since the compensating species for CT solution in C_4AF and C_2F is the oxygen interstitial, CT more readily disolves in reduced C_2F

$$2CT + V_O^{\bullet\bullet} + Fe_{Fe(o)}^{\times} \xrightarrow{\Delta H = -1.34\,eV} 2Ca_{Ca}^{\times} + Ti_{Fe(o)}^{\bullet} + Fe_{Fe(t)}^{\times} + 6O_O^{\times}$$

and in reduced C_4AF

$$2CT + V_O^{\bullet\bullet} + Fe_{Fe(o)}^{\times} \xrightarrow{\Delta H = -1.20\,eV} 2Ca_{Ca}^{\times} + Ti_{Fe(o)}^{\bullet} + Fe_{Al(t)}^{\times} + 6O_O^{\times}.$$

This means that the amount of dissolved CT depends markedly on the degree to which the ferrite phase is reduced. That is, the solution is predicted to show significant dependence on the partial pressure of oxygen.

3.3. Cluster formation in C_4AF

Solution of CT in C_4AF introduces O_i'' and $Ti_{Fe(o)}^{\bullet}$ defects which may cluster and thereby lower the solution energy of CT. The favoured arrangement of defects in

the cluster can be determined by calculating the cluster geometry that has the lowest solution energy.

The favoured cluster in C_4AF is $\{Ti^{\bullet}_{Fe(o)} : O''_i : Ti^{\bullet}_{Al(t)}\}^{\times}$, which has a solution energy of 1.22 eV per titanium ion (compared to 1.72 eV without clustering). The most stable configuration of the $\{Ti^{\bullet}_{Fe(o)} : O''_i : Ti^{\bullet}_{Al(t)}\}^{\times}$ cluster in C_4AF is shown in Fig. 1c. Note that now cluster formation is considered and the preferred solution mechanism includes a titanium ion on a tetrahedral Al site. Essentially, the oxygen interstitial ion with its associated titanium ions results in the local lattice being somewhat reminiscent of the solute CT phase, since the coordination of the former tetrahedral Al site has been increased.

The solution energy is lowered further when two clusters bind together. This leads to the formation of an octahedrally coordinated titanium ion at the former tetrahedral aluminum site since there are now two oxygen interstitials adjacent to this site. This cluster, a $\{Ti^{\bullet}_{Fe(o)} : O''_i : Ti^{\bullet}_{Al(t)} : Ti^{\bullet}_{Fe(o)} : O''_i : Ti^{\bullet}_{Al(t)}\}^{\times}$ complex, is illustrated in Fig. 1d. It has a titanium ion in the octahedral sites immediately above and below the new octahedrally coordinated titanium ion (at the former tetrahedral Al site). An additional adjacent titanium in what remains a tetrahedral site completes the cluster. This cluster has a corresponding solution energy of 0.96 eV per titanium ion. If a third $\{Ti^{\bullet}_{Fe(o)} : O''_i : Ti^{\bullet}_{Al(t)}\}^{\times}$ cluster is adjacent to the two cluster complex the solution energy is reduced further to 0.87 eV per titanium ion. Such defect clustering is reminiscent of the triple octahedral planes in the $Ca_4Fe_2Ti_2O_{11}$ structure proposed by Prasanna and Navrotsky [12]. This therefore provides a possible connection between titanium ordering in the ferrite phase and the structures of intermediate phases in the ferrite-calcium titanate system. However, such a picture is inconsistent with the structure proposed for $Ca_3Fe_2TiO_8$ [12] which has only double octahedral planes.

Under reducing conditions C_4AF contains $Fe'_{Al(t)}$ defects which are compensated by $V^{\bullet\bullet}_O$. If defect cluster formation occurs, the most stable defect cluster is $\{Fe'_{Fe(o)} : V^{\bullet\bullet}_O : Fe'_{Fe(o)}\}$ in which the Fe^{2+} ion now resides on an iron site. Solution of CT in the reduced material results in the presence of $Ti^{\bullet}_{Fe(o)}$ which becomes the compensating defect for the $Fe'_{Al(t)}$ defects present under reducing conditions. These defects may also form clusters, $\{Fe'_{Al(t)} : Ti^{\bullet}_{Fe(o)}\}$. Solution of CT in the reduced material, assuming clustering, should therefore be written,

$$2CT + \{Fe'_{Fe(o)} : V^{\bullet\bullet}_O : Fe'_{Fe(o)}\} + Fe^{\times}_{Fe(o)} \longrightarrow 2Ca^{\times}_{Ca} + 2\{Fe'_{Al(t)} : Ti^{\bullet}_{Fe(o)}\} + 6O^{\times}_O$$

In this case, the solution energy is -0.43 eV, not as favourable as the case where cluster formation was assumed to not occur. This is because the $\{Fe'_{Fe(o)} : V^{\bullet\bullet}_O : Fe'_{Fe(o)}\}$ cluster binding energy is more than twice that of the $\{Fe'_{Al(t)} : Ti^{\bullet}_{Fe(o)}\}$ defect. Nevertheless the solution energy is still negative, and solution of CT is greatly enhanced under reducing conditions.

TABLE IV Summary of lowest energy CT solution mechanisms

compound	solution energy (eV per Ti)	compensating defect
α-Al_2O_3	4.69	Ca'_{Al}
CA	3.79	O''_i
C_3A	2.76	V''_{Ca}
α-Fe_2O_3	2.33	Fe'_{Fe}
CF	1.78	Fe'_{Fe}
C_4AF	1.72	O''_i
C_2A	1.65	O''_i
C_2F	1.51	O''_i

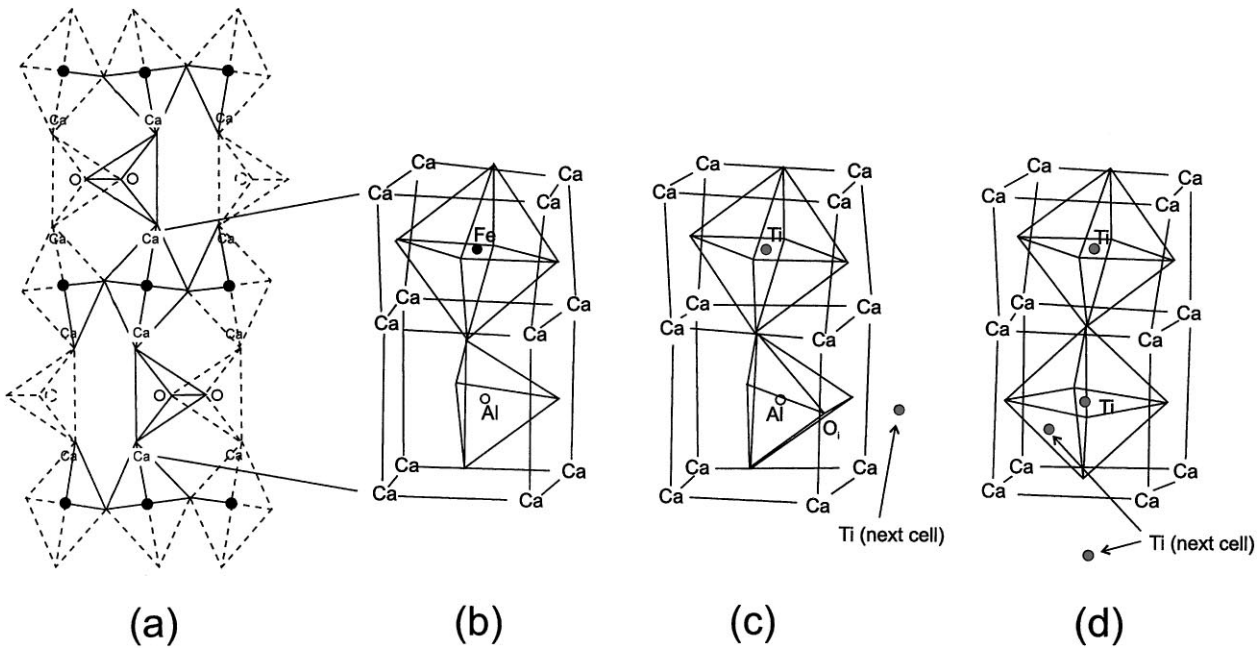

Figure 1 Solution of CT in C_4AF, (a) b-c projection of a single unit cell showing the position of (b) one eighth of a unit cell, (c) the structure of a $\{Ti^{\bullet}_{Fe(o)} : O''_i : Ti^{\bullet}_{Al(t)}\}^{\times}$ cluster and (d) a $\{Ti^{\bullet}_{Fe(o)} : O''_i : Ti^{\bullet}_{Al(t)} : Ti^{\bullet}_{Fe(o)} : O''_i : Ti^{\bullet}_{Al(t)}\}^{\times}$ cluster.

4. Conclusions

The relative values of the calculated CT solution energies in Al_2O_3, Fe_2O_3, CF, C_2F, CA, C_2A, C_3A, and C_4AF are consistent with finding titanium primarily in the ferrite phases rather than the other compounds listed. In addition, the simulations indicate that in all cases, titanium substitutes for trivalent host cations, and the compensating defects vary from compound to compound. The calculated solution energies and compensating defects are summarized in Table IV.

Several more detailed conclusions regarding the ferrite phase can also be made:

- In the dilute limit titanium clearly favours the octahedral site in the ferrite phase.
- Under reducing conditions Ti solution in the ferrite phase is greatly enhanced.
- When Fe reduction does not occur defect cluster formation significantly reduces the solution energy.
- The most stable defect cluster geometries closely resemble the arrangement of ions in the solute CT lattice.

Acknowledgements

This research has been supported through funding from Lafarge. The authors wish to acknowledge Gerdjan Busker for his maintenance of the computing facilities, which were provided in part through EPSRC grant GR/K74302, and Licia Minervini for help in preparing the manuscript.

References

1. A. GLOTER, J. INGRIN, D. BOUCHER, K. SCRIVENER and C. COLLIEX, *Physics and Chemistry of Minerals*, in press.
2. A. GLOTER, Ph.D. thesis, Universite de Paris-Sud 2000.
3. T. FÜLLMANN, G. WALENTA, T. BIER, B. ESPINOSA and K. SCRIVENER, *World Cement (Research)*, June 1999.
4. A. M. HARRISSON, H. F. W. TAYLOR and N. B. WINTER, *Cem, Concr. Res.* **15** (1985) 775.
5. J. D. DUNITZ and L. E. ORGEL, *J. Phys. Chem. Solids* **3** (1957) 20.
6. B. G. DICK and A. W. OVERHAUSER, *Phys. Rev.* **112** (1958) 90.
7. M. O. ZACATE and R. W. GRIMES, *J. Mater. Sci.* **34** (1999) 445.
8. L. MINERVINI and R. W. GRIMES, *J. Phys. and Chem. of Solids* **60** (1999) 235.
9. M. A. MCCOY, R. W. GRIMES and W. E. LEE, *Phil. Mag. A* **75** (1997) 833.
10. C. R. A CATLOW and A. M. STONEHAM (eds.), *J. Chem. Soc. Faraday Trans.* (special issue) 85 (1989).
11. M. LESLIE, SERC Daresbury Laboratory Report DL/SCI/TM31T, Science and Engineering Research Council, Daresbury, U.K., 1982.
12. T. R. S. PRASANNA and A. NAVROTSKY, *J. Mater. Res.* **9** (1994) 3121.
13. D. R. LIDE (ed.), "CRC Handbook of Chemistry and Physics," 2nd ed., (CRC Press, Inc., Boca Raton, 1996).
14. K. P. HUBER and G. HERZBERG, "Molecular Spectra and Molecualr Structure IV. Constants of Diatomic Molecules" (Van Nostrand, New York, 1979).
15. J. H. HARDING and N. C. PYPER, *Phil. Mag. Letters* **71** (1995) 113.
16. R. W. GRIMES, D. J. BINKS and A. B. LIDIARD, *Phil. Mag. A* **72** (1995) 651.
17. R. W. GRIMES, *J. Am. Ceram. Soc.* **77** (1994) 378.
18. R. W. G. WYCKOFF, "Crystal Structures, Vol. 2," 2nd ed., (Interscience Publishers, New York, 1964) p. 394.
19. B. A. WECHSLER and C. T. PREWITT, *American Mineralogist* **69** (1984) 176.
20. H. J. A KOOPMANS, G. M. H. VAN DE VELDE and P. J. GELLINGS, *Acta Cryst.* **C39** (1983) 1323.
21. R. W. G. WYCKOFF, "Crystal Strucutres, Vol. 3," 2nd ed., (Interscience Publishers, New York, 1965) p. 297.
22. B. MOROSIN and R. W. LYNCH, *Acta Cryst.* **B28** (1972) 1040.

Received 6 October 1999
and accepted 10 February 2000